

# Controlling the start of combustion on an HCCI Diesel engine

Mathieu HILLION, Jonathan CHAUVIN, and Nicolas PETIT

**Abstract**—In this paper we propose a control strategy to improve stability of the combustion of HCCI engines during sharp transients. This approach complements existing airpath and fuelpath controllers, and aims at accurately controlling the start of combustion (*soc*). For that purpose, injection time is adjusted based on a simple Knock Integral Model and real time intake manifold signals. Experimental results are presented, which stress the relevance of the approach.

## I. INTRODUCTION

In the context of environmental restrictions and sustainable development, pollution standards have become more and more stringent over the last 15 years. Engine pollutant emission reduction has then become a topic of major interest for engine development. Lately, two main strategies have been explored: namely after-treatment and improved combustion modes. For Diesel engines, cost of after treatment devices are usually high. In turn, this has spurred a major interest in developments of cleaner combustion modes such as the Highly Premixed Combustion modes (HPC), including Homogeneous Charge Compression Ignition (HCCI).

Consider a Diesel engine with a turbocharger and an Exhaust Gas Recirculation (EGR) as depicted in Figure 1. This engine can be used in various combustion modes ranging from conventional to homogeneous. In this paper, we focus on the HCCI mode which is the most challenging from a control perspective (see [1] and [2]).

HCCI combustion requires the use of high Exhaust Gas Recirculation (EGR) rates. The air charge admitted in the cylinder is significantly diluted, which reduces nitrogen oxides ( $\text{NO}_x$ ) emissions by lowering the temperature peak during combustion. This combustion takes place according to the timeline detailed in Figure 2. There are two main phases corresponding to the airpath subsystem (which involves the intake manifold, the intake throttle, the turbocharger, and the EGR valve) and the fuelpath subsystem (which consists of the injectors). This combustion mode is highly sensitive. Accurate airpath control and fuelpath controllers are thus required to manage the HCCI combustion.

Airpath controllers have long been proposed (see [3], [4] and their references). They result in efficient tracking of the intake manifold variables (reference total mass, composition, and temperature of the intake charge) even during transients.

M. Hillion (corresponding author) is a PhD Candidate in Mathematics and Control, Centre Automatique et Systèmes, École des Mines de Paris, 60, bd St Michel, 75272 Paris, France.

J. Chauvin is with the Department of Engine Control in Institut Français du Pétrole, 1 & 4 Avenue de Bois Préau, 92852 Rueil Malmaison, France.

N. Petit is with the Centre Automatique et Systèmes, École des Mines de Paris, 60, bd St Michel, 75272 Paris, France.

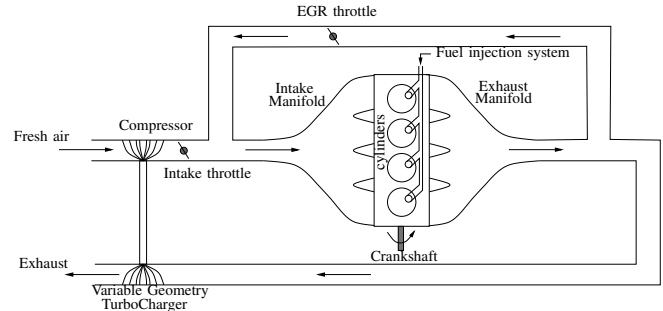


Fig. 1. Scheme of a direct injection HCCI engine with EGR and Turbocharger

Usually, three main actuators are employed (EGR valve, intake throttle and turbocharger).

Classic fuelpath controllers can be described as follows. During the cylinder compression phase, fuel is injected and mixed to the compressed air and burned gas mixture. The fuel vaporizes and, eventually, auto-ignites after the so-called ignition delay (see Figures 2 and 3). Standard fuelpath control strategies focus on controlling each cylinder fuel mass. This is usually sufficient to produce a reference torque, *provided that the combustion actually takes place*.

As we will now discuss it, these controllers are often not sufficient to stabilize the HCCI combustion mode during transients. In fact, and by contrast to conventional Diesel combustion mode, slight offsets of cylinder initial conditions (e.g. pressure, temperature, or composition) easily cause problems. In practice, if the airpath controller and the fuelpath controller are not coordinated, combustion stability is jeopardized during transients. More precisely, the combustion phenomenon is stable but its basin of attraction is so small that transient phases easily lead to instabilities. This is clearly visible in Figure 5 where combustion timings are reported. Large overshoots or undershoots reflect the fact that the combustion is not stabilized during transients. In fact, this can easily lead to stall. This can be seen in Figure 4 where experimentally observed misfire is reported (at time 30s). In details, one can see in Figure 4a that the produced torque drastically drops during transient resulting in stall. This occurs every time this transient trajectory is tracked. In fact, the engine is artificially restarted by the test bench generator at a high frequency. In the setup used to obtain these results, a classic airpath and fuelpath control strategy is considered. Our focus is on developing an improved method capable of achieving the desired transients. To address the discussed issues, i.e. to circumvent changes in the cylinder initial conditions, we propose to use the *injection time* as an

actuator to control the start of combustion. This is the main contribution of this paper. A noticeable point of our approach is that this control variable can be used on all commercial line engines without requiring any hardware upgrade. Controlling the start of combustion (*soc*) is an efficient strategy in the presented context of HCCI engines, because, instead of a classic flame propagation phenomenon, spatially distributed starts of combustion are simultaneously observed in the chamber.

In this paper, we consider three parameters as cylinder initial conditions: these are the pressure, the temperature and the composition. We assume that the *soc* is defined by a Knock Integral Model (KIM) (see [5], [6] or [7]). In practical implementation, the initial conditions are either inferred from direct measurements or estimated by an external observer. To guarantee that the *soc* occurs at a desired setpoint, we update the injection time according to a first order development of the KIM. As already mentioned controlling the *soc* represents a first step toward more general active combustion control methods. Other interesting possibilities could include the control of numerous scheduling variables such as the middle of combustion. They are the subject of on-going research.

The paper is organized as follows. In Section II, we detail existing combustion control technologies that we wish to complement and present our approach. In Section III, we present the KIM we base our study on, along with the main physical assumptions underlying our work. In Section IV, we formulate the control problem, and propose a solution at first order in Section V. Experimental results obtained on a 2.2 liter four cylinder direct injection engine are reported and discussed in Section VI. Conclusions and future direction are given in Section VII.

## II. CURRENT COMBUSTION CONTROLLERS AND PROPOSED IMPROVEMENT

A complete nomenclature of engine variables is given in Table I. In generally observed engine setups, airpath and fuelpath controllers are used to guarantee that engine variables (pressures, temperatures, and injected fuel mass among others) track reference values. These controllers are used in the context of actual vehicle implementation which imply frequent transients due to varying driver torque demands ( $\overline{IMEP}$ ) and engine speed ( $N_e$ ). In turn, these demands result in frequent transients for reference airpath and fuelpath variables. Typical histories of setpoint signals  $\overline{P}_{intake}$ ,  $\overline{X}$ ,  $\overline{\theta}_{soi}$ ,  $\overline{m}_{inj}$  are reported in Figure 4. While both controllers seems to work simultaneously, stall is very often observed during transients. This clearly appears in Figure 4a (stall occurs every time this transient trajectory is tracked). We now give some insight into this phenomenon. In open loop, the airpath and the fuelpath subsystems have slow and fast dynamics, respectively. In closed loop, the airpath subsystem cannot be rendered arbitrarily fast. The culprits are the turbocharger inertia and recirculation hold-ups. Neglecting fuelpath transients, injection parameters are instantaneously set to values corresponding to the targeted

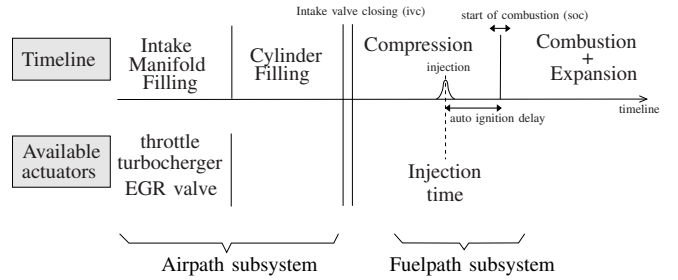


Fig. 2. Timeline of Diesel engine cycle with direct injection

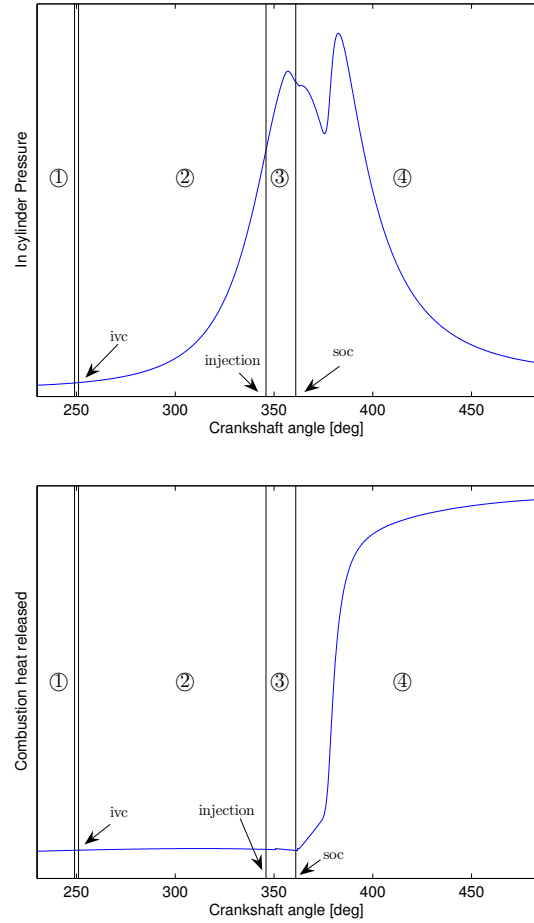


Fig. 3. Experimental results: In-cylinder pressure during one cycle and the associated combustion heat release: ① filling the cylinder, ②: compression, ③: auto ignition, ④: Combustion and expansion, *ivc*: intake valve closing, *soc*: start of combustion. (360 corresponds to the Top Dead Center)

steady states ( $(\overline{\theta}_{soi}, \overline{m}_{inj}) = f(\overline{IMEP}, N_e)$ ). While this strategy is sufficient in conventional Diesel mode, this is not the case in HCCI mode. A typical scenario is as follows. Figure 4 shows a torque transient on a 4-cylinder HCCI engine using this injection strategy. In Figures 4b and 4c, it appears that the airpath controller regulates the intake manifold pressure and BGR around their reference values. Tracking is not instantaneous though and regulation errors appear in transients. Bias in steady state are mainly due to calibration problems. BGR lag (appearing at time 81s) is due to EGR valve clogging. These airpath regulation errors are

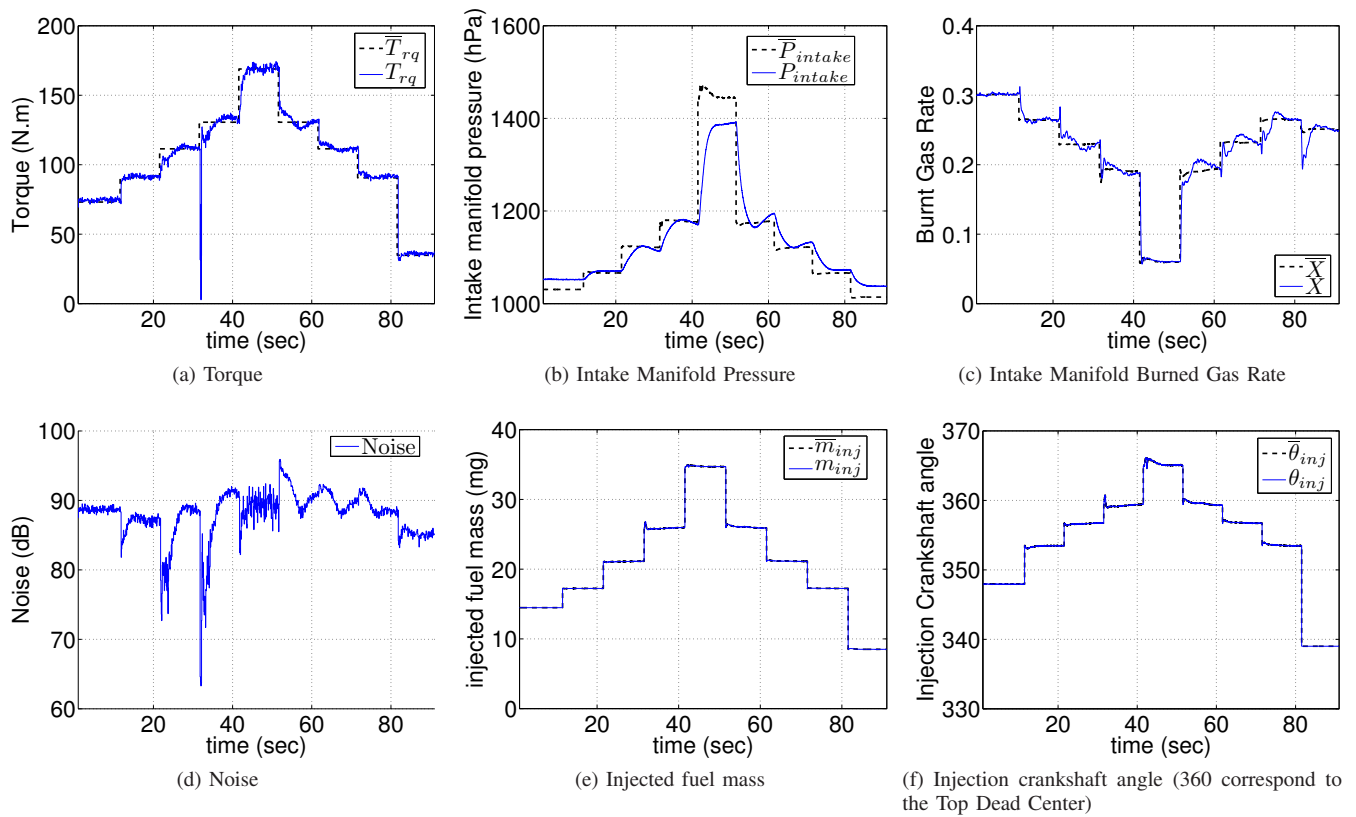


Fig. 4. Experimental results on a 4-cylinder HCCI engine with direct injection. Charge transient at constant speed of 1400rpm with standard fuelpath strategy.

not interfering with the presented work. On the other hand, fuel injection timing and fuel mass are instantaneously set to reference values corresponding to the targeted steady states (see 4e and 4f)<sup>1</sup>. Finally, Figures 4a and 4d stress that this

<sup>1</sup>at time 31s a minor overshoot appears on the fuelpath setpoints while the torque demand is constant. In fact, due to the torque output drop at this time, the engine speed temporarily decreases (the test bed engine speed regulator fails) which makes the engine control system to change the setpoints

TABLE I  
NOMENCLATURE

Symb.	Quantity	Unit
$\theta$	Crankshaft angle	-
$V$	Cylinder volume	$m^3$
$P(\theta)$	Cylinder pressure	$Pa$
$T(\theta)$	Cylinder temperature	$K$
$X$	In-cylinder burned gas rate (BGR)	-
$V_{ivc}$	In-cylinder volume at <i>ivc</i>	$m^3$
$P_{ivc}$	Cylinder pressure at <i>ivc</i>	$Pa$
$T_{ivc}$	Cylinder temperature at <i>ivc</i>	$K$
$\phi$	Air/fuel ratio	-
$\theta_{soi}$	Injection crankshaft angle	-
$\theta_{soc}$	Start of combustion crankshaft angle	-
$m_{inj}$	Injected fuel mass	$mg$
$\gamma$	Ratio of specific heat	-
$IMEP$	Torque	$Nm$
$N_e$	Engine speed	$rpm$

strategy, and the corresponding mismatch between airpath and fuelpath variables, lead to important additional noise and stall during transients.

#### Possible upgrades

As detailed earlier in the introduction, controlling the combustion is the key to HCCI engine control. Two main timing variables permit to sketch the quality of the combustion. These are the *soc* and the middle of the combustion. One often assume that if these timing variables are efficiently controlled, the combustion will takes place in a desired way. The *soc* is difficult to measure and is often replaced on experimental test benches by the  $CA_{10}$  ( $CA_X$  is defined as the cranshaft angle where X-per-cent of the fuel as been burned which are post-reconstructed from in-cylinder pressure measurements). The middle of the combustion is defined as the  $CA_{50}$ . Figure 5 shows that the existing fuelpath control strategies fail to efficiently stabilize  $CA_{10}$  and  $CA_{50}$  to their tracked steady-state value. Combustion occurs then too early or too late, leading to instabilities, stall, and large noise variations. To correct this, different solutions have been proposed to control the  $CA_{50}$  or the *soc*. We now sketch an overview of the litterature.

In [8], Haraldsson *et al.* present closed-loop combustion control using Variable Compression Ratio (VCR) as actuator. Changing the compression ratio directly impacts on the rise of pressure and temperature in the cylinder during compression, making differences in thermodynamic conditions at the

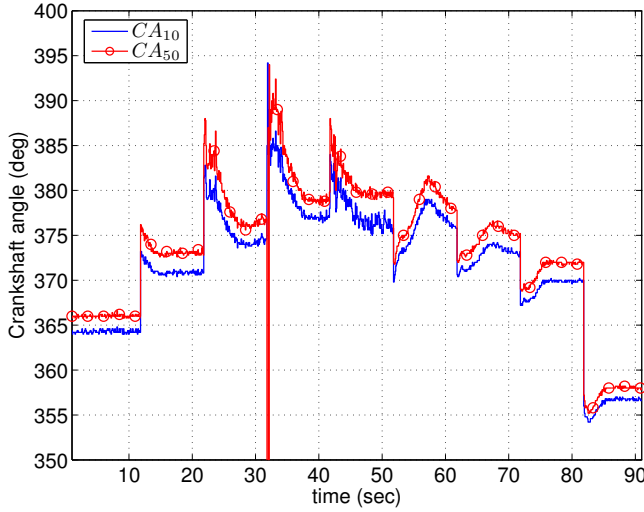


Fig. 5. Evolution of the  $CA_{10}$  (time closed to the start of combustion) and the  $CA_{50}$  (middle of the combustion) during the transient presented in Figure 4 (360 corresponds to the Top Dead Center).

injection time. The whole combustion process is then delayed or advanced.

In [9], Olsson *et al.* present a dual-fuel solution. These two fuels have different auto-ignition properties. Taking advantage of this,  $soc$  can be regulated by changing the recipe of the mixture to be injected.

In [10], [11] or [12] the authors present HCCI control results based on a Variable Valve Train (VVT) actuation, which allows to trap hot exhaust gases in the cylinder from one cycle to the next. The charge temperature can thus be modified. This internal recirculation is used to control auto-ignition time.

#### Proposed upgrade

All the controllers presented in the previous Section use high frequency in-cylinder sensors and/or additional actuators (VCR, dual-fuel system, VVT). Such technical solutions are costly. Rather, to control the  $soc$ , we propose a solution requiring only devices available on all commercial-line engines, *i.e.* requiring no cylinder pressure sensors.

Consider the fuelpath subsystem whose dynamic behavior, as previously discussed, is inconsistent with the dynamic behavior of the airpath subsystem. This subsystem is controlled by the fuel injection. The injected mass is used to produce a reference torque and it cannot be changed without jeopardizing performance. Therefore, only one degree of freedom of the fuelpath remains as possible additional control variable. It is the injection time (start of injection) which appears in the combustion timeline in Figure 2.

In our approach, we propose to cascade the control of the  $soc$  onto the injection time  $\theta_{soi}$  variable. This implies that, instead of constant values corresponding to references,  $\theta_{soi}$  has non-constant values during transients. A particular phenomenon has to be accounted for. Due to the varying auto ignition delay,  $\theta_{soi}$  does not directly initiate the combustion (this is rather different from spark advance in spark ignited

engines). In fact, combustion takes place after the auto ignition delay, due to evaporation and mixing of the fuel and chemical activation. This lag can be estimated. Our control strategy is based on an ignition delay model, and, thus, does not need any in-cylinder sensors. It is in fact open loop. This model involves physical parameters of the gases aspirated in the combustion chamber (*i.e.* BGR, temperature, pressure, air/fuel ratio) and parameters of the fuel injection (*i.e.* injection crankshaft angle, injected fuel mass).

### III. MODELLING

#### A. Knock Integral Model

The main equation we rely our work on is the KIM which is usually used to predict the auto ignition delay of fuel/air/burned-gases mixture (see [5], [6] or [7]). This model gives an implicit relation between  $\theta_{soi}$ ,  $\theta_{soc}$  and the physical in-cylinder parameters such as  $P(\theta)$ ,  $T(\theta)$ ,  $X$  (additionally an air/fuel ratio  $\phi$  can be considered), usually found under the implicit integral form

$$\int_{\theta_{soi}}^{\theta_{soc}} \mathcal{A}(p(\theta)) \frac{d\theta}{N_e} = 1 \quad (1)$$

where  $\mathcal{A}$  is an Arrhenius function, and  $p(\theta) = (P(\theta), T(\theta), X)^T$ . Our control strategy can be used with any (smooth) function  $\mathcal{A}$ . A prime example is (see [13])

$$\mathcal{A}(p(\theta)) = \frac{A}{1 + CX} P(\theta)^n \exp\left(-\frac{T_A}{T(\theta)}\right) \quad (2)$$

where  $A$ ,  $C$ ,  $n$ , and  $T_A$  are known constant positive parameters. This formula is used throughout the paper and experiments. Numerous other possible choices could be considered as well, using the same approach.

#### B. Relating the Knock Integral to available measurements

The proposed model (1)-(2) is expressed in terms of in-cylinder thermodynamics quantities ( $P(\theta)$ ,  $T(\theta)$ , and  $X$ ) which are not directly measured on commercial line engines. Therefore, we rewrite it in terms of different parameters. To compute the in-cylinder pressure ( $P(\theta)$ ) and in-cylinder temperature ( $T(\theta)$ ) during compression, we assume that a static relation holds. In particular, the transformation is considered isentropic. Classically, during this isentropic transformation,  $PV^\gamma$  and  $TV^{\gamma-1}$  are both constant. In these relations,  $V$  represents the cylinder volume, which is perfectly known as a function of the crankshaft angle  $\theta$ . This thermodynamic assumption (see *e.g.* [14]) is supported by the fact that, during compression, gas temperature is much lower than it is during combustion. In short, during the compression phase, wall heating losses are neglected.

We consider the  $ivc$  (intake valve closing) values as initial conditions for the isentropic transformation. These are assumed equal to the intake manifold temperature and pressure right before  $ivc$  which are both measured. These

considerations yield

$$P(\theta) = P_{ivc} v_{ivc}(\theta)^\gamma \quad (3)$$

$$T(\theta) = T_{ivc} v_{ivc}(\theta)^{\gamma-1} \quad (4)$$

$$\text{with } v_{ivc}(\theta) \triangleq \frac{V(\theta_{ivc})}{V(\theta)}$$

Finally, in (2),  $X$  is assumed constant from the *ivc* to the *soc*. This is not unrealistic, because no chemical reaction takes place between *ivc* and *soc*. Its value is obtained from an observer presented in [3].

Substituting equations (3) and (4) into (1), the auto ignition model takes the form

$$\int_{\theta_{soi}}^{\theta_{soc}} \mathcal{A}_{ivc}(p_{ivc}, \theta) \frac{d\theta}{N_e} = 1 \quad (5)$$

with  $p_{ivc} \triangleq (P_{ivc}, T_{ivc}, X)$   
 $\mathcal{A}_{ivc}(p_{ivc}, \theta) \triangleq \mathcal{A}(p(\theta))$

Equation (5) summarizes the influence of the values of the physical parameters at *ivc* on the start of combustion. In particular, (2) becomes

$$\mathcal{A}_{ivc}(p_{ivc}, \theta) = \frac{A}{1 + CX} P_{ivc}^n v_{ivc}(\theta)^{n\gamma} \exp\left(-\frac{T_A}{T_{ivc} v_{ivc}(\theta)^{\gamma-1}}\right) \quad (6)$$

#### IV. CONTROL PROBLEM

At steady state, all the  $p_{ivc} \triangleq (P_{ivc}, T_{ivc}, X)$  parameters are stabilized by the airpath controller to their reference values ( $\bar{p}_{ivc}$ ). Further, the injection timing  $\theta_{soi}$  is directly set to its reference value ( $\bar{\theta}_{soi}$ ) by the fuelpath controller. A reference combustion takes place. The corresponding reference  $\bar{\theta}_{soc}$  satisfies

$$\int_{\bar{\theta}_{soi}}^{\bar{\theta}_{soc}} \mathcal{A}_{ivc}(\bar{p}_{ivc}, \theta) \frac{d\theta}{N_e} = 1 \quad (7)$$

During transient,  $\delta p \triangleq p_{ivc} - \bar{p}_{ivc} \neq 0_{\mathbb{R}^3}$ . If fuel is injected at the reference time  $\theta_{soi}$ , then the start of combustion differs from the reference combustion one. We propose to compensate any such known error  $\delta p$  with a corrective offset  $\delta\theta_{soi}$  on the injection time reference  $\bar{\theta}_{soi}$  so that the actual  $\theta_{soc}$  can equal  $\bar{\theta}_{soc}$ . We can summarize this in the following problem:

*Problem 1:* Given  $\bar{\theta}_{soi}$ ,  $\bar{p}_{ivc}$  and  $\bar{\theta}_{soc}$  satisfying (7), consider  $\delta p \in \mathbb{R}^3$ . Find  $\delta\theta_{soi}$  such that

$$\int_{\bar{\theta}_{soi} + \delta\theta_{soi}}^{\bar{\theta}_{soc}} \mathcal{A}_{ivc}(\bar{p}_{ivc} + \delta p, \theta) \frac{d\theta}{N_e} = 1 \quad (8)$$

#### V. SOLUTION AT FIRST ORDER

It might be difficult to find an explicit solution to Problem 1 when considering Arrhenius functions of the general

form (6). A simple way to proceed is to look for an approximate solution. Equation (7) and (8) yield

$$\int_{\bar{\theta}_{soi} + \delta\theta_{soi}}^{\bar{\theta}_{soc}} \mathcal{A}_{ivc}(\bar{p}_{ivc} + \delta p, \theta) \frac{d\theta}{N_e} = \int_{\bar{\theta}_{soi}}^{\bar{\theta}_{soc}} \mathcal{A}_{ivc}(\bar{p}_{ivc}, \theta) \frac{d\theta}{N_e}$$

$$\int_{\bar{\theta}_{soi}}^{\bar{\theta}_{soc}} \mathcal{A}_{ivc}(\bar{p}_{ivc} + \delta p, \theta) - \mathcal{A}_{ivc}(\bar{p}_{ivc}, \theta) \frac{d\theta}{N_e} = \int_{\bar{\theta}_{soi}}^{\bar{\theta}_{soi} + \delta\theta_{soi}} \mathcal{A}_{ivc}(\bar{p}_{ivc}, \theta) \frac{d\theta}{N_e} + o(\delta\theta_{soi}, \delta p)$$

At first order, this gives

$$\mathcal{A}_{ivc}(\bar{p}_{ivc}, \theta) \frac{\delta\theta_{soi}}{N_e} = \int_{\bar{\theta}_{soi}}^{\bar{\theta}_{soc}} \left( \frac{\partial \mathcal{A}_{ivc}}{\partial p_{ivc}}(\bar{p}_{ivc}, \theta) \delta p \right) \frac{d\theta}{N_e}$$

The required correction is

$$\delta\theta_{soi} = \frac{1}{\mathcal{A}_{ivc}(\bar{p}_{ivc}, \theta)} \left( \int_{\bar{\theta}_{soi}}^{\bar{\theta}_{soc}} \frac{\partial \mathcal{A}_{ivc}}{\partial p_{ivc}}(\bar{p}_{ivc}, \theta) d\theta \right) \delta p \quad (9)$$

In practice, this correction is easily computable, because  $\mathcal{A}_{ivc}$ ,  $\bar{p}_{ivc}$ ,  $\delta p$ ,  $\bar{\theta}_{soi}$ , and  $\bar{\theta}_{soc}$  are all known.

In details, the respective influences of offsets in *ivc* pressure, temperature, and composition in the case of the model presented in (2) are as follows (this can easily be extended to any other auto ignition model)

$$\delta\theta_{soi} = \frac{1}{\mathcal{A}_{ivc}(\bar{p}_{ivc}, \theta)} (\alpha_P \delta P_{ivc} + \alpha_T \delta T_{ivc} + \alpha_X \delta X) \quad (10)$$

with

$$\alpha_P = \int_{\bar{\theta}_{soi}}^{\bar{\theta}_{soc}} \frac{\partial \mathcal{A}_{ivc}}{\partial P_{ivc}}(\bar{p}_{ivc}, \theta) d\theta = \frac{n}{\bar{P}_{ivc}} > 0 \quad (11)$$

$$\alpha_T = \int_{\bar{\theta}_{soi}}^{\bar{\theta}_{soc}} \frac{\partial \mathcal{A}_{ivc}}{\partial T_{ivc}}(\bar{p}_{ivc}, \theta) d\theta = \frac{T_A}{\bar{T}_{ivc}^2} \int_{\bar{\theta}_{ivc}}^{\bar{\theta}_{soc}} \mathcal{A}_{ivc}(\bar{p}_{ivc}, \theta) v_{ivc}^{1-\gamma}(\theta) d\theta > 0 \quad (12)$$

$$\alpha_X = \int_{\bar{\theta}_{soi}}^{\bar{\theta}_{soc}} \frac{\partial \mathcal{A}_{ivc}}{\partial X}(\bar{p}_{ivc}, \theta) d\theta = -\frac{C}{1 + CX} < 0 \quad (13)$$

The signs of the correction parameter  $\alpha_P$ ,  $\alpha_T$ , and  $\alpha_X$  are intuitive. If the pressure error ( $\delta P$ ) or temperature error ( $\delta T$ ) are positive (with the composition error equal to zero,  $\delta X = 0$ ), meaning that the pressure or the temperature at the *ivc* are higher than the reference, the mixture would auto-ignite too soon. This is counterbalanced by the positive injection crankshaft angle correction (see the sign of (11) and (12)). If the composition error ( $\delta X$ ) is positive (with  $\delta P = \delta T = 0$ ), meaning that the burned gas rate is higher than the reference, the mixture is more diluted, which increases the auto ignition delay. In such cases, the *soc* would thus be too late. This is counterbalanced by the negative injection crankshaft angle correction (see the sign of (13)).

TABLE II  
EXPERIMENTAL SETUP

Bore $\times$ Stroke	87.0 $\times$ 92.0 mm
Number of cylinders	4
Compression ratio	14.0:1
Displacement	2.2 Liters
Injection device	Solenoid
Maximum injection pressure	1600 bar
Piston bowl design	NADI™
Intake Valve Closing	$\theta_{ivc} = 232\text{deg}$ (360 is Top Dead Center)

## VI. EXPERIMENTAL RESULTS

### A. Experimental setup

All experimental results presented in the following have been obtained on a four cylinder direct injection Diesel engine running in HCCI combustion mode. Exact specifications are reported in Table II. The engine is an upgrade of a turbocharged multi-cylinder commercial line engine. A high pressure EGR circuit is used. It extracts hot burned gases upstream of the turbine and introduces them downstream of the compressor. A valve allows the EGR rate to be controlled (see Figure 1). Finally, both the air and the EGR circuits include an air cooler to keep the intake manifold temperature around 330K.

### B. Controller design

The general control scheme is presented in Figure 6. It includes the strategy proposed in this article to control the *soc*. This new strategy is included in the dark-grey box “correction calculation” which implements equations (10)-(13). In this setup, the injection crankshaft angle  $\theta_{soi}$  is not simply set to its reference value  $\bar{\theta}_{soi}$  but is corrected according to the airpath errors  $\delta p$ .

The model (2) is used in the controller design. This model has been calibrated on 50 points of the whole engine operating range using classical optimisation method.

The controller has been integrated in the complete IFP engine control system already developed in Matlab/Simulink. RTW (Real Time Workshop) and xPC target toolboxes are used for real time code generation. The task execution time of the proposed controller is about 20  $\mu\text{s}$  on a AMD 4.8Ghz target.

### C. Results

Figure 7 reports experimental results. The scenario is a varying torque demand at constant engine speed of 1400 rpm. For sake of comparisons, the torque trajectory is the same as the one used in Section II (Figure 4).

The torque trajectory is presented in Figure 7a. As mentioned in Section II, the airpath control regulates the intake manifold pressure and BGR around their reference values in order to meet torque demands (see Figure 7b and 7c). The not instantaneous tracking of these reference values make the new fuelpath controller correct the injection crankshaft angle reference value (see Figure 7f). The injection crankshaft

angle sent to the injectors is then different from its reference value. Despite the fact that torque reference trajectory are the same in scenarios of Figures 4 and 7, slight mismatches can be observed in reference trajectories (comparing dark dashed line in Figures b, c, e, and f). This is caused by slight influences of the proposed fuelpath controller on the exhaust conditions (mainly pressure and temperature) which has an impact on the intake conditions via the EGR and turbocharger physical loops (see future published work).

Improvements in engine torque response are shown in Figure 7a. In fact, one can remark that stall has been avoided. During increasing torque transients, intake manifold pressure is lower than its reference and BGR is higher than its reference, both errors leading to a longer auto ignition time than the reference. Without injection crankshaft angle correction, the *soc* occurs too late which makes the combustion very close to the instability. With the new fuelpath controller, the injection occurs sooner (see Figure 7f). The *soc* and combustion are then closer to their reference, stall is thus avoided (during decreasing torque transients, the exact symmetric scenario occurs). Secondly, torque response during transients is much faster with the proposed upgrade (the reader can compare Figure 4a and 7a around 20s).

The engine noise transients have been improved too. With the classical fuelpath strategy, noise level varies a lot during torque demand transitions. On the other hand, with the proposed correction strategy, noise transients happen faster and over and undershoots are much smaller or even disappear (see Figure 7d). One can thus reasonably expect improvements in acoustic comfort.

At last, Figure 8 presents the evolution of the  $CA_{10}$  and  $CA_{50}$  during the torque trajectory of the Figure 7. In comparison to Figure 5, the proposed strategy stabilizes much quicker the combustion timing. Combustion, even during transients, seems then to be much closer to the reference one (at least timing is). This clearly proves that the strategy proposed in section V and implemented in Section VI answers the control problem 1.

## VII. CONCLUSION AND FUTURE WORK

An improvement for the fuelpath control strategy of HCCI diesel engine has been presented. Instead of directly setting the injection crankshaft angle to its reference value, we propose to synchronize the fuelpath to the airpath. This controller is mainly based on the linearization of an auto ignition delay model (KIM). Provided an estimation of in-cylinder conditions at the *ivc* (which in our case is inferred from intake manifold signals), this method is very general. It can be applied to engine with external or internal Gas recirculation, to naturally aspirated engine, throttled engines and/or with turbochargers.

The presented experimental results stress the relevance of this new approach. Stall problems during transients are solved and combustion stability (one great challenge in HCCI combustion mode) is improved. At the light of these results, controlling the *soc* seems to be an appropriate solution to improve the stability of the HCCI combustion.

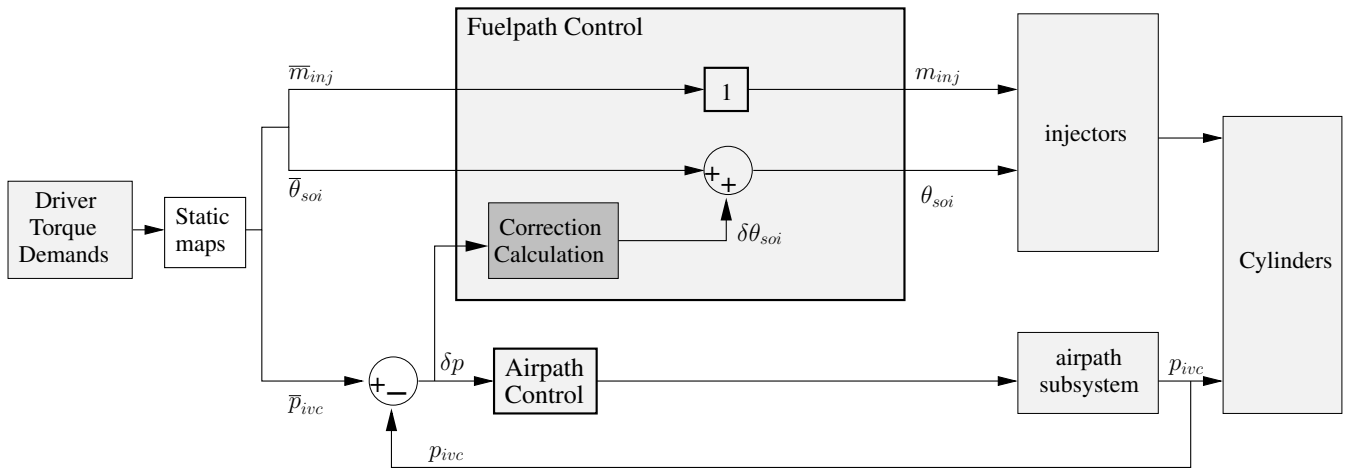


Fig. 6. Design of the new control strategy. The dark grey block has been added, counterbalancing airpath errors  $\delta p$  with an injection crankshaft angle offset.

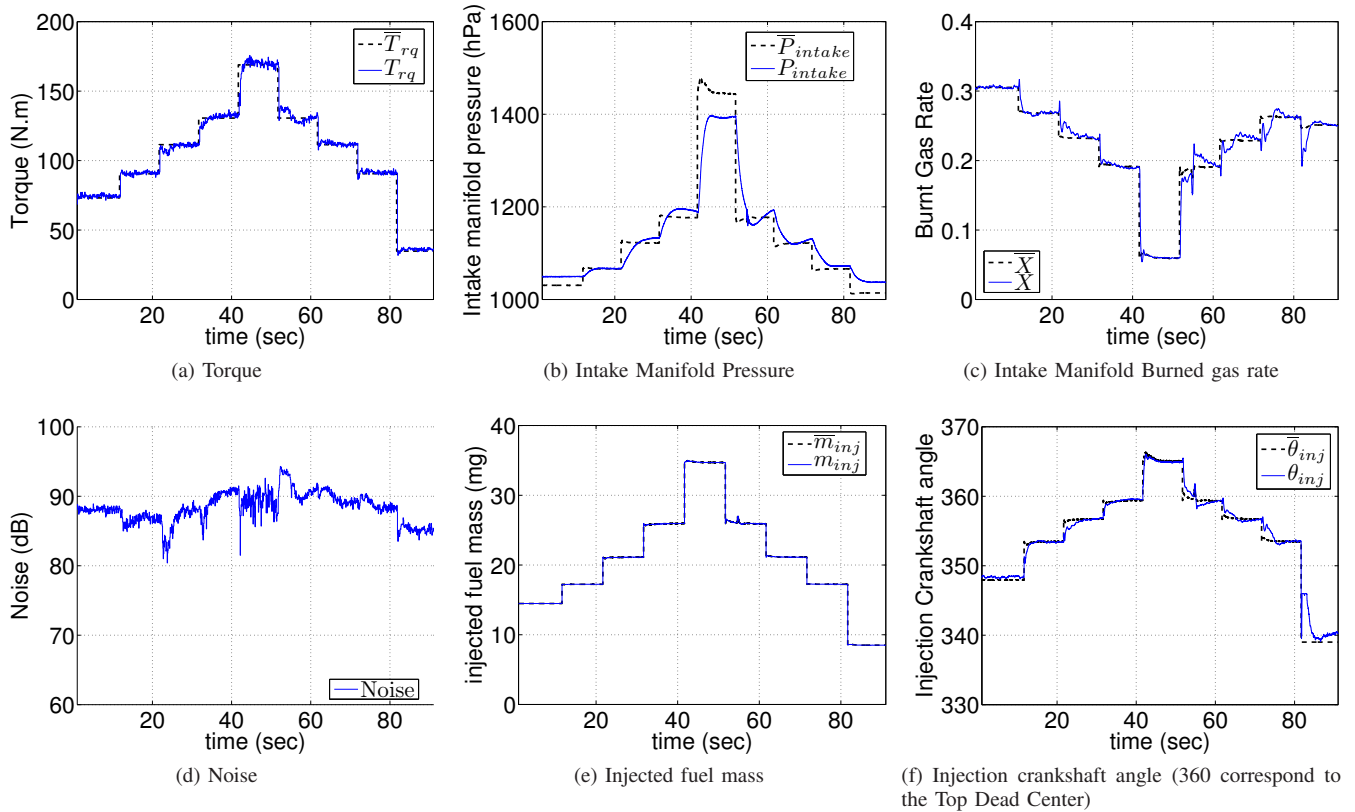


Fig. 7. Experimental results on a 4-cylinder HCCI engine with direct injection. Charge transient at constant speed of 1400rpm with the new fuelpath control strategy.

A next step is to complement this feed-forward control strategy with a feedback control based on combustion timing measurements which could be provided, for instance, by accelerometers.

## VIII. AKNOWLEDGEMENT

The authors would like to gratefully thank Gilles Corde for his scientific support.

## REFERENCES

- [1] J. Kahrstedt, K. Behnk, A. Sommer, and T. Wormbs, "Combustion processes to meet future emission standards," in *Motortechnische Zeitschrift*, 2003, pp. 1417–1423.
- [2] B. Walter and B. Gatellier, "Near zero NOx emissions and high fuel efficiency diesel engine: the NADI<sup>TM</sup> concept using dual mode combustion," in *Oil and Gas Science and Technology*, vol. 58, 2003, pp. 101–114.
- [3] J. Chauvin, G. Corde, and N. Petit, "Transient control of a Diesel engine airpath," in *American Control Conference*, 2007.
- [4] —, "Constrained motion planning for the airpath of a Diesel HCCI engine," in *Conference on Decision and Control*, 2006.

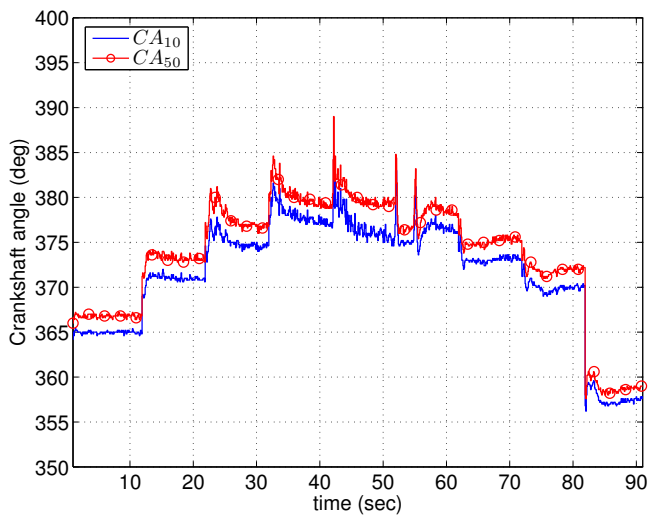


Fig. 8. Evolution of the  $CA_{10}$  and the  $CA_{50}$  during the transient presented in Figure 7 (360 correspond to the Top Dead Center).

- [5] K. Swan, M. Shahbakhti, and C. Koch, "Predicting start of combustion using a modified knock integral method for an HCCI engine," in *Proc. SAE World Congress*, no. 2006-01-1086, 2006.
- [6] J. Livengood and P. Wu, "Correlation of auto ignition phenomena in internal combustion engines and rapid compression machine," in *Fifth International Symposium on Combustion*, 1955, pp. 347–356.
- [7] J. Heywood, *Internal combustion engine fundamental*. Mc Graw-Hill, Inc, 1988.
- [8] G. Haraldsson, P. Tunestål, B. Johansson, and J. Hyvonen, "HCCI combustion phasing with closed-loop combustion control using variable compression ratio in a multi cylinder engine," in *Proc. SAE World Congress*, no. 2003-01-1830, 2003.
- [9] J.-O. Olsson, P. Tunestål, and B. Johansson, "Closed-loop control of an HCCI engine," in *Proc. SAE World Congress*, no. 2001-01-1031, 2001.
- [10] C. Chiang, A. G. Stefanopoulou, and M. Jankovic, "Nonlinear observer-based control of load transitions in homogeneous charge compression ignition engines," in *IEEE Transaction on Control System Technology*, vol. 15, no. 3, may 2007.
- [11] K. Chang, G. Lavoie, and A. Babajimopoulos, "Control of a multi-cylinder HCCI engine during transient operation by modulating residual gas fraction to compensate for wall temperature effects," in *Proc. SAE World Congress*, no. 2007-01-0204, 2007.
- [12] H.-E. Angström, B. Eriksson, and J. Wikander, "Transient control of HCCI through combined intake and exhaust valve actuation," in *Proc. SAE World Congress*, no. 2003-01-3172, 2003.
- [13] F.-A. Lafossas, M. Marbaix, and P. Menegazzi, "Development and application of a 0D D.I. Diesel combustion model for emissions prediction," in *Proc. SAE World Congress*, no. 2007-01-1841, 2007.
- [14] D. J. Rausen, A. G. Stefanopoulou, J.-M. Kang, J. A. Eng, and T.-W. Kuo, "A mean-value model for control of homogeneous charge compression ignition (HCCI) engines," in *IEEE Proceedings of American Control Conference*, 2004.